Majorana Fermions and Exotic Surface Andreev Bound States in Topological Superconductors: Application to Cu#Bi_2Se_3

Majorana Fermions and Exotic Surface Andreev Bound States in Topological Superconductors: Application to $Cu_xBi_2Se_3$

Timothy H. Hsieh[1] and Liang Fu[1,2]

[1]*Department of Physics, Massachusetts Institute of Technology, Cambridge, Massachusetts 02139, USA*
[2]*Department of Physics, Harvard University, Cambridge, Massachusetts 02138, USA*

(Received 15 September 2011; published 8 March 2012)

The recently discovered superconductor $Cu_xBi_2Se_3$ is a candidate for three-dimensional time-reversal-invariant topological superconductors, which are predicted to have robust surface Andreev bound states hosting massless Majorana fermions. In this work, we analytically and numerically find the linearly dispersing Majorana fermions at $k = 0$, which smoothly evolve into a new branch of gapless surface Andreev bound states near the Fermi momentum. The latter is a new type of Andreev bound states resulting from both the nontrivial band structure and the odd-parity pairing symmetry. The tunneling spectra of these surface Andreev bound states agree well with a recent point-contact spectroscopy experiment [S. Sasaki *et al.*, Phys. Rev. Lett. **107**, 217001 (2011)] and yield additional predictions for low temperature tunneling and photoemission experiments.

DOI: 10.1103/PhysRevLett.108.107005 PACS numbers: 74.20.Rp, 73.43.−f, 74.20.Mn, 74.45.+c

The discovery of topological insulators has generated much interest in not only understanding their properties and potential applications to spintronics and thermoelectrics but also searching for new topological phases. A particularly exciting avenue is topological superconductors [1–9], in which unconventional pairing symmetries lead to topologically ordered superconducting ground states [10–12]. The hallmark of a topological superconductor is the existence of gapless surface Andreev bound states which host itinerant Bogoliubov quasiparticles. These quasiparticles are solid-state realizations of massless Majorana fermions.

There is currently an intensive search for topological superconductors. In particular, a recently discovered superconductor $Cu_xBi_2Se_3$ with $T_c \sim 3$ K [13] has attracted much attention [14]. A theoretical study [10] proposed that the strong spin-orbit coupled band structure of $Cu_xBi_2Se_3$ favors an odd-parity pairing symmetry, which leads to a time-reversal-invariant topological superconductor in three dimensions. Subsequently, many experimental and theoretical efforts [15–19] have been made towards understanding superconductivity in $Cu_xBi_2Se_3$. In a very recent point-contact spectroscopy experiment, Sasaki *et al.* [20] have observed a zero-bias conductance peak which strongly indicates unconventional pairing [21].

In this Letter, we find a new branch of gapless surface Andreev bound states (SABS), in addition to linearly dispersing Majorana fermions at $\mathbf{k} = 0$, in the topological superconducting phase of $Cu_xBi_2Se_3$ and related doped semiconductors. This new branch of SABS is located near the Fermi momentum and is protected by a new bulk topological invariant. Moreover, they result in unique features in the tunneling spectra which are in good agreement with the point-contact spectroscopy experiment on $Cu_xBi_2Se_3$ [20]. We conclude by predicting clear signatures of these SABS, which can be tested in future tunneling and photoemission experiments at low temperatures.

We start from the $k \cdot p$ Hamiltonian for the band structure of $Cu_xBi_2Se_3$ near Γ [10]:

$$H(\mathbf{k}) = m\sigma_x + v_z k_z \sigma_y + v\sigma_z(k_x s_y - k_y s_x). \quad (1)$$

Here $\sigma_z = \pm 1$ labels the two Wannier functions which are primarily p_z orbitals (from Se and Bi atoms) on the upper and lower part of the quintuple layer (QL) unit cell, respectively (see Fig. 1). Each orbital has a twofold spin degeneracy labeled by $s_z = \pm 1$. We note that an earlier $k \cdot p$ Hamiltonian [22] violates the mirror symmetry of the lattice, and a corrected version [23] is consistent with (1). Detailed discussion of the discrepancy is left to the Supplemental Material [24]. The sign of mv_z is a crucial quantity which will now be inferred from the existence of

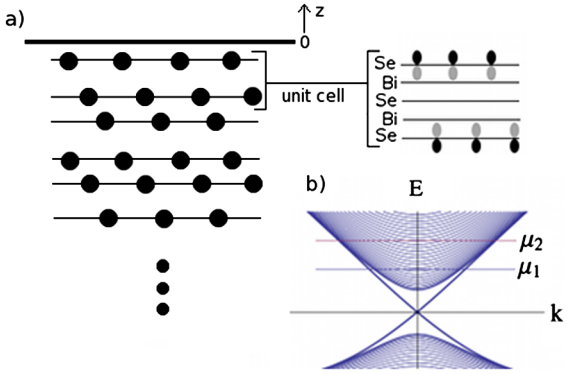

FIG. 1 (color online). (a) Side view of a semi-infinite crystal of Bi_2Se_3. The two relevant p_z orbitals are shown in the zoom-in view of the QL unit cell. (b) Bulk and surface bands of the tight-binding model for Bi_2Se_3. μ_1 and μ_2 denote two chemical potentials where the surface states have, respectively, not merged and merged into the bulk bands.

surface states near $k_x = k_y = 0$ in the surface Brillouin zone.

Consider a semi-infinite $Cu_xBi_2Se_3$ crystal occupying $z < 0$, which is naturally cleaved between QLs (see Fig. 1). The realistic boundary condition corresponding to such a termination in the continuum $k \cdot p$ theory is [10]

$$\sigma_z \psi(z = 0) = \psi(z = 0). \tag{2}$$

This boundary condition reflects the vanishing of the electron wave function on the bottom layer ($\sigma_z = -1$) at $z = 0$. Solving the differential equation

$$E\psi = H(k_x, k_y, -i\partial_z)\psi \tag{3}$$

subject to (2), we find two branches of midgap states

$$\psi_\pm(k_x, k_y, z) = e^{z/l}(1, 0)_\sigma \otimes (1, \pm ie^{i\phi})_s, \tag{4}$$

where $l = -v_z/m$ is the decay length, ϕ is the azimuthal angle of (k_x, k_y), and the subscripts σ and s denote the orbital σ_z and spin s_z basis. For $v_z m > 0$, there are no decaying solutions; only when $v_z m < 0$ in (4) do we obtain surface states decaying in the $-z$ direction. The dispersion of these surface states is $E_\pm(k_x, k_y) = \pm v\sqrt{k_x^2 + k_y^2} \equiv \pm vk$, which agree well with the photoemission data from $Cu_xBi_2Se_3$ [15]. Thus, the existence of surface states on surfaces terminated between QLs establishes $v_z m < 0$ in $H(\mathbf{k})$ for $Cu_xBi_2Se_3$ [24].

Having established that $v_z m < 0$ and v parametrizes the linear dispersion of the surface states, we now turn to the superconducting state of $Cu_xBi_2Se_3$. Reference [10] classified four different pairing symmetries compatible with short-range pairing interactions, and found that a spin-triplet, orbital-singlet, odd-parity pairing symmetry is favored when the interorbital attraction exceeds the intraorbital one. The mean-field Hamiltonian of this superconducting state is

$$\begin{aligned} H_{\mathrm{MF}} &= \int d\mathbf{k}[c_{\mathbf{k}}^\dagger, \bar{c}_{-\mathbf{k}}]\mathcal{H}(\mathbf{k})\begin{bmatrix} c_{\mathbf{k}} \\ \bar{c}_{-\mathbf{k}}^\dagger \end{bmatrix}, \\ \mathcal{H}(\mathbf{k}) &= (H(\mathbf{k}) - \mu)\tau_z + \Delta\sigma_y s_z \tau_x. \end{aligned} \tag{5}$$

Here $c_{\mathbf{k}}^\dagger = (c_{\mathbf{k},1\uparrow}^\dagger, c_{\mathbf{k},1\downarrow}^\dagger, c_{\mathbf{k},2\uparrow}^\dagger, c_{\mathbf{k},2\downarrow}^\dagger)$ and $\bar{c}_{-\mathbf{k}} \equiv c_{-\mathbf{k}} \cdot is_y$ are four-component electron operators, with the subscripts 1, 2 labeling the two orbitals [Fig. 1(a)]. In the Bogoliubov–de Gennes (BdG) Hamiltonian $\mathcal{H}(\mathbf{k})$, τ_x and τ_z are Pauli matrices in Nambu space, Δ is the pairing potential, and $\mu > |m|$ is the chemical potential in the conduction band.

The above odd-parity superconducting $Cu_xBi_2Se_3$ is fully gapped in the bulk but has topologically protected surface Andreev bound states. To determine the wave function and dispersion of these bound states, we begin by solving the BdG Hamiltonian $\mathcal{H}(k_x, k_y, -i\partial_z)$ for the SABS at $k_x = k_y = 0$. We find a Kramers pair of $\epsilon = 0$ eigenstates [24]:

$$\begin{aligned} \psi_{k=0,\alpha}(z) = e^{z\cdot\Delta/|v_z|}&(\sin(k_F z - \theta), \sin(k_F z))_\sigma \\ &\otimes [(1, -\alpha)_s, i\,\mathrm{sgn}(v_z)(1, \alpha)_s]_\tau, \\ \alpha &= \pm 1. \end{aligned} \tag{6}$$

Here $k_F \equiv \sqrt{\mu^2 - m^2}/v_z$ is Fermi momentum in the z direction, and θ is defined by $e^{i\theta} = (m + i\sqrt{\mu^2 - m^2})/\mu$. The subscript τ denotes a Nambu spinor. The Bogoliubov quasiparticle at $k = 0$ is defined by $\gamma_\alpha = \int dz \psi_{k=0,\alpha}(z)(c^\dagger(z), \bar{c}(z))_{k=0}^T$. It is straightforward to verify that $\gamma_\alpha^\dagger = \gamma_\alpha$ up to an unimportant overall phase. This means that such quasiparticles are two-component massless Majorana fermions in $2 + 1$ dimensions.

Having found the SABS wave function at $\epsilon = 0$, $k = 0$, we now show that the SABS dispersion crosses $\epsilon = 0$ again at finite k, which is one of the main results of this Letter. We establish this second crossing in two different ways: first, by a direct calculation, and second, by a topological argument. It will become evident that the two approaches yield complementary information.

In the direct approach, we search for a second crossing by asking for which $k_0 > 0$ does $\mathcal{H}(0, k_0, -i\partial_z)\psi = 0$ have a solution (it suffices to consider $k_x = 0$, $k_y \equiv k_0 > 0$ only, due to rotational invariance). We find that k_0 is the nontrivial solution of the algebraic equation [24]

$$|x|^2 + 2\,\mathrm{sgn}(v_z)\frac{E_F}{m}\,\mathrm{Re}(x) - 1 = 0, \tag{7}$$

where x is defined as

$$x \equiv \frac{vk_0 - i(\Delta + iE_F)}{\sqrt{(vk_0)^2 + (\Delta + iE_F)^2}}, \qquad E_F \equiv \sqrt{\mu^2 - m^2}. \tag{8}$$

For $Cu_xBi_2Se_3$ in the normal state with $\Delta = 0$ and $v_z m < 0$, the above equation has a solution $k_0 = \mu/v$, which exactly corresponds to the topological insulator surface states at Fermi energy obtained earlier in (4). With superconductivity, topological surface states in the normal state turn into SABS, with their location k_0 and wave function $\psi_{k_0,\alpha}$ perturbed by Δ: $k_0 \simeq \frac{\mu}{v}(1 - \frac{\Delta^2}{2m^2})$ and $\psi_{k_0,\alpha}$ acquires particle-hole mixing to first order in Δ. Because of rotational invariance of the $k \cdot p$ Hamiltonian, the second crossing, hereafter denoted by k_0, exists along all directions in the xy plane. This leads to a Fermi surface of SABS.

In the topological approach, we first solve for the SABS dispersion at small k and use topological arguments to infer its behavior at large k. Again, we set $k_x = 0$ for convenience. Treating the k_y-dependent term in H_{BdG} as a perturbation, we find the dispersion is linear near $k = 0$: $\epsilon_\alpha(k) = \alpha\tilde{v}k + o(k^3)$, forming a Majorana cone. The velocity $\tilde{v}$ is given by

$$\tilde{v} = v\frac{\Delta^2 + \mathrm{sgn}(v_z)\Delta m}{\Delta^2 + \mathrm{sgn}(v_z)\Delta m + \mu^2} \simeq v\,\mathrm{sgn}(v_z)\frac{m\Delta}{\mu^2}. \tag{9}$$

In the second equality, we have used the fact $\Delta \ll |m| < \mu$ for weak-coupling superconductors.

In (9), it is important that the SABS velocity $\tilde{v}$ at $k = 0$ has an opposite sign from the band velocity v in the normal state of the doped topological insulator $Cu_xBi_2Se_3$ ($v_z m < 0$). As we now show, this fact has crucial implications for the SABS dispersion away from $k = 0$: the two branches of SABS $\psi_{k,\pm}$ must cross each other at $\epsilon = 0$ an odd number of times between $\bar{\Gamma}$ and the surface Brillouin zone edge $\bar{M}$. The existence of such additional crossings is dictated by a topological invariant we call "mirror helicity," which is a generalization of mirror Chern number [25] in topological insulators to topological superconductors. To define this invariant, note that the crystal structure of $Cu_xBi_2Se_3$ has a mirror reflection symmetry $x \to -x$. As a result, the band structure (1) is invariant under mirror. However, the pairing potential in (5) changes sign under mirror reflection. So the BdG Hamiltonian is invariant under a mirror reflection combined with a Z_2 gauge transformation $\Delta \to -\Delta$:

$$\mathcal{H}(k_x, k_y, k_z) = \tilde{M}\mathcal{H}(-k_x, k_y, k_z)\tilde{M}^{-1}. \quad (10)$$

Here $\tilde{M} = M\tau_z$, $M = -is_x$ represents mirror reflection on electron spin. Because of this generalized mirror symmetry, bulk states are grouped into two classes with mirror eigenvalues $\pm i$, respectively. Each class can have a nonzero Chern number $n_{\pm i}$. Time-reversal symmetry requires $n_{+i} = -n_{-i}$. The magnitude $|n_{+i}| = |n_{-i}|$ determines the number of helical Andreev modes with $k_x = 0$ on the edge of the yz plane, while the sign defines a Z_2 mirror helicity: $\eta \equiv \mathrm{sgn}(n_{+i}) = -\mathrm{sgn}(n_{-i})$. The bulk topological invariant η determines the helicity of such Andreev modes. For instance, $\eta < 0$ implies that the mode with mirror eigenvalue $-i$ ($+i$) moves clockwise (anticlockwise) with respect to the $+x$ axis at the edge of the yz plane, and its energy-momentum dispersion curve must eventually merge into the $E > 0$ bulk quasiparticle continuum at a large positive (negative) momentum. Similar bulk-boundary correspondence applies to surface states in topological insulators [25,26].

As we show in the Supplemental Material [24], the topological superconducting phase of $Cu_xBi_2Se_3$ and the undoped topological insulator Bi_2Se_3 have the same mirror helicity η, which is determined by the sign of the Dirac band velocity v in the bulk. Given the relation between η and helicity of surface excitations, this implies that the SABS in $Cu_xBi_2Se_3$ must have the same helicity as surface states in Bi_2Se_3. On the other hand, the SABS velocity $\tilde{v}$ at $k = 0$ has an opposite sign from the Dirac band v. To reconcile this fact with the helicity requirement, the two SABS branches $\psi_{k,\alpha}$—which are mirror eigenstates with eigenvalues $\tilde{M} = i\alpha$—must become twisted and switch places before merging into the bulk. This necessarily results in an odd number of crossings between $\bar{\Gamma}$ and $\bar{M}$.

The above topological argument reveals the robustness of gapless SABS at the second crossing in the $k \cdot p$ regime and beyond. In the $k \cdot p$ regime, the surface states at $\mathbf{k}$ and $-\mathbf{k}$ have opposite mirror eigenvalues (or spins) due to their helical nature, whereas the pairing symmetry Δ only pairs states with the same mirror eigenvalues. This symmetry incompatibility makes the surface states remain gapless in the topological superconducting phase [27]. Moreover, the topological argument demonstrates that the second crossing is topologically protected by the mirror helicity invariant in the bulk, as long as $\tilde{v}/v < 0$ at $k = 0$. As a result, the second crossing remains in a much larger energy range, even when higher order corrections to the $k \cdot p$ Hamiltonian become important, as shown below. In particular, we emphasize that the existence of the second crossing is independent of whether surface states are separated from the bulk at the Fermi energy.

To gain more insight into these twisted SABS and to calculate their local density of states, we explicitly obtain its dispersion in the entire surface Brillouin zone. For this purpose, we construct a two-orbital tight-binding model in the rhombohedral lattice shown in Fig. 1 and calculate the SABS dispersion numerically. Details of our tight-binding model and its distinction from previous models [19,20] are described in the Supplemental Material [24].

Here we would like to note the following aspects of our model. The normal state tight-binding model is constructed to reproduce both the $k \cdot p$ Hamiltonian (1) of $Cu_xBi_2Se_3$ in the small k limit and the boundary condition (2) in the continuum theory. The bulk and surface bands of the normal state tight-binding model are displayed in Fig. 1(b); at chemical potential μ_1, the Fermi momentum is relatively small and terms higher order than $\mathbf{k}$ are negligible, whereas at μ_2, these higher order terms cause deviation from the $k \cdot p$ Hamiltonian.

Upon adding odd-parity superconductivity pairing to the model, we obtain the SABS dispersion (Fig. 2). A branch of linearly dispersing Majorana fermions is found at $k = 0$, which signifies a three-dimensional topological superconductor. In addition, the bands of Andreev bound states in the surface Brillouin zone are twisted: they connect the Majorana fermion at $k = 0$ with the second crossing near Fermi momentum. Such behavior was independently found by Hao and Lee [19,24], and its topological origin is revealed by our analytical calculations and arguments.

For a given branch ($\tilde{M} = \pm i$) of SABS, its particle-hole character evolves as a function of momentum from having an equal amount of particle and hole (charge neutral) at $k = 0$ to being exclusively hole or particle (charged) at large k. At chemical potential μ_1, the SABS near the second crossing can be identified with nearly unpaired surface states in the normal state, which show up twice—as particle and hole—in the BdG spectrum. However, even when these surface states have merged into the bulk, the SABS still has the second crossing, as required by the

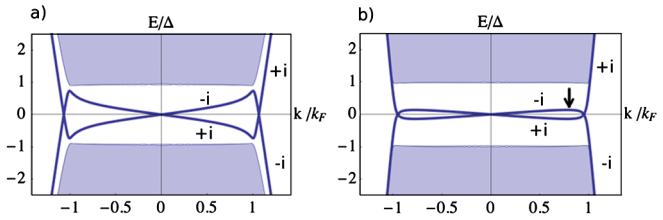

FIG. 2 (color online). SABS dispersion for the tight-binding model in which (a) $m = -0.3 < 0$, $\mu_1 = 0.6$ and (b) $m = -0.3 < 0$, $\mu_2 = 1$. The mirror eigenvalues are displayed near each branch of SABS. The SABS twist with a second crossing near Fermi momentum, as also observed in Ref. [19]. The arrow denotes where the dispersion has zero slope, resulting in a van Hove singularity in the density of states.

mirror helicity. This is shown in Fig. 2(b), at chemical potential μ_2. The resulting gapless SABS near the second crossing has substantially more particle-hole mixing than the first case and is unrelated to surface states in the normal state. Such SABS defy a quasiclassical description and represent a new type of Andreev bound states which arises from the interplay between nontrivial band structure and unconventional superconductivity.

Finally, we relate our findings of SABS in $Cu_xBi_2Se_3$ to the recent point-contact spectroscopy experiment [20], in which a zero-bias differential conductance peak along with a dip near the superconducting gap edge was observed below 1.2 K and attributed to SABS. To compare with this experiment, we calculate the local tunneling density of states (LDOS) as a function of energy for $m/\mu_2 = 0.3$—roughly the value found in angle-resolved photoemission spectroscopy (ARPES) [15]. The resulting LDOS at zero and finite temperatures are shown in Fig. 3. The finite temperature LDOS from $T = 0.05\Delta$ to $T = 0.2\Delta$ agrees with the experimentally observed differential conductance peaks as well as the dips with the slight asymmetry between positive and negative voltages. Both features along with the absence of coherence peaks contrast sharply with the tunneling spectrum of an s-wave superconductor.

In addition to comparison with the experiment, we make the following predictions stemming from the zero temperature LDOS in Fig. 3(a). Here the two peaks arise from van Hove singularities at the particular energy near $E = 0$ where the SABS bands have zero slope, indicated by the

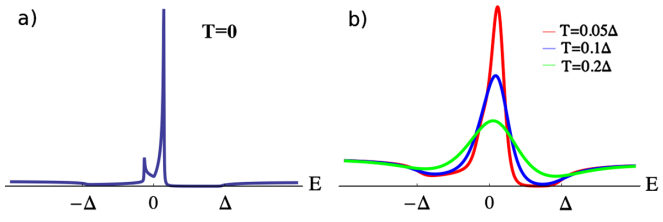

FIG. 3 (color online). Tunneling local density of states (arbitrary units) at (a) $T = 0$ and (b) finite temperature. In both cases, the chemical potential is $\mu_2 = 1$.

arrow in Fig. 2(b). Furthermore, the significant asymmetry in the height of these two peaks reflects the fact that the SABS at the turning point is primarily of hole type, as noted earlier. The energy of these two peaks and the magnitude of their asymmetry depends somewhat on details of band structure. However, the existence of two peaks only depends on there being a turning point in the SABS dispersion, which is guaranteed by the existence of a second crossing in a wide regime of chemical potentials. Hence, we predict that for relatively clean surfaces the zero-bias conductance peak in the tunneling spectra will split into two asymmetric peaks at even lower temperatures. Such peaks will be an unambiguous signature of Majorana fermions smoothly turning into normal surface electrons. Furthermore, the SABS dispersion we predict in Fig. 2 can be directly tested in future ARPES experiments.

While the main focus of this Letter is $Cu_xBi_2Se_3$, we end by discussing the implications of our findings for superconducting doped semiconductors with similar band structures. Candidates include Bi_2Te_3 [28] under pressure, $TlBiTe_2$[29], PbTe [30], SnTe [31], and GeTe [32]. Provided that the material is inversion symmetric and its Fermi surface is centered at time-reversal-invariant momenta, the Dirac-type relativistic $k \cdot p$ Hamiltonian (1) describes their band structures [33]. Moreover, if the pairing symmetry is odd under spatial inversion and fully gapped, the system is (almost) guaranteed to be a topological superconductor according to our criterion [10,34]. Our work is also relevant to noncentrosymmetric superconductors such as YPtBi [35], if their pairing symmetries have dominant odd-parity components.

As a final point which captures the essence of this work, we compare and contrast SABS in doped superconducting topological insulators with normal insulators, which differ by a band inversion ($v_z m < 0$ versus $v_z m > 0$). In both, the Majorana fermion SABS exist at $k = 0$ as shown in (6) and (9). However, the SABS in doped normal insulators do not necessarily have the second crossing near Fermi momentum [24]. This can be understood from our mirror helicity argument, with the difference being that $\tilde{v}/v > 0$ for $v_z m > 0$ [see Eq. (9)]. In this sense, the new type of surface Andreev bound state and its phenomenological consequences are the unique offspring of both nontrivial band structure and odd-parity topological superconductivity.

We thank Yoichi Ando, Erez Berg, Chia-Ling Chien, Patrick Lee, and Yang Qi for helpful discussions, as well as Anton Akhmerov and David Vanderbilt for helpful comments on the manuscript. This work is supported by U.S. DOE under cooperative research agreement Contract No. DE-FG02-05ER41360 and NSF Graduate Research Fellowship under Grant No. 0645960 (T. H.), and the Harvard Society of Fellows and MIT startup funds (L. F.). L. F. would like to thank Institute of Physics in China and Institute of Advanced Study at Tsinghua University for generous hosting.

Note added.—Two recent studies [19,20] calculated the surface spectral function numerically in $Cu_xBi_2Se_3$ tight-binding models. The second crossing of SABS was independently found in Ref. [19]. We also learned of another point-contact measurement on $Cu_xBi_2Se_3$ [36].

[1] A. P. Schynder, S. Ryu, A. Furusaki, and A. W. W. Ludwig, Phys. Rev. B **78**, 195125 (2008).
[2] A. Kitaev, arXiv:0901.2686.
[3] N. Read and D. Green, Phys. Rev. B **61**, 10267 (2000).
[4] R. Roy, arXiv:0803.2868.
[5] X. L. Qi, T. L. Hughes, S. Raghu, and S. C. Zhang, Phys. Rev. Lett. **102**, 187001 (2009).
[6] M. M. Salomaa and G. E. Volovik, Phys. Rev. B **37**, 9298 (1988); M. A. Silaev and G. E. Volovik, J. Low Temp. Phys. **161**, 460 (2010).
[7] S. K. Yip, J. Low Temp. Phys. **160**, 12 (2010).
[8] S. Ryu, J. E. Moore, and A. Ludwig, Phys. Rev. B **85**, 045104 (2012).
[9] K. Nomura, S. Ryu, A. Furusaki, and N. Nagaosa, Phys. Rev. Lett. **108**, 026802 (2012).
[10] L. Fu and E. Berg, Phys. Rev. Lett. **105**, 097001 (2010).
[11] X. L. Qi, T. L. Hughes, and S. C. Zhang, Phys. Rev. B **81**, 134508 (2010).
[12] M. Sato, Phys. Rev. B **81**, 220504(R) (2010).
[13] Y. Hor *et al.*, Phys. Rev. Lett. **104**, 057001 (2010).
[14] P. A. Lee, http://www.condmatjournalclub.org/?p=833
[15] L. A. Wray *et al.*, Nature Phys. **6**, 855 (2010); Phys. Rev. B **83**, 224516 (2011).
[16] M. Kriener *et al.*, Phys. Rev. Lett. **106**, 127004 (2011).
[17] M. Kriener *et al.*, Phys. Rev. B **84**, 054513 (2011).
[18] P. Das *et al.*, Phys. Rev. B **83**, 220513(R) (2011).
[19] L. Hao and T. K. Lee, Phys. Rev. B **83**, 134516 (2011).
[20] S. Sasaki *et al.*, Phys. Rev. Lett. **107**, 217001 (2011).
[21] For reviews on surface Andreev bound states in unconventional superconductors, see S. Kashiwaya and Y. Tanaka, Rep. Prog. Phys. **63**, 1641 (2000); G. Deutscher, Rev. Mod. Phys. **77**, 109 (2005).
[22] H. Zhang *et al.*, Nature Phys. **5**, 438 (2009).
[23] C. X. Liu *et al.*, Phys. Rev. B **82**, 045122 (2010).
[24] See Supplemental Material at http://link.aps.org/supplemental/10.1103/PhysRevLett.108.107005 for details.
[25] J. C. Y. Teo, L. Fu, and C. L. Kane, Phys. Rev. B **78**, 045426 (2008).
[26] R. Takahashi and S. Murakami, Phys. Rev. Lett. **107**, 166805 (2011).
[27] Strictly speaking, mirror helicity protects the second crossing along the mirror-invariant line ΓM only. However, higher order terms which reduce the full rotational symmetry are small.
[28] J. L. Zhang *et al.*, Proc. Natl. Acad. Sci. U.S.A. **108**, 24 (2010).
[29] R. A. Hein and E. M. Swiggard, Phys. Rev. Lett. **24**, 53 (1970).
[30] Y. Matsushita *et al.*, Phys. Rev. B **74**, 134512 (2006).
[31] R. Hein, Phys. Lett. **23**, 435 (1966).
[32] R. A. Hein *et al.*, Phys. Rev. Lett. **12**, 320 (1964).
[33] L. Fu and C. L. Kane, Phys. Rev. B **76**, 045302 (2007).
[34] Y. Qi and L. Fu (to be published).
[35] N. P. Butch *et al.*, Phys. Rev. B **84**, 220504 (2011).
[36] T. Kirzhner *et al.*, arXiv:1111.5805